

The behavior of non-linear anisotropies in bouncing Bianchi I models of loop quantum cosmology

Dah-Wei Chiou^{1,*} and Kevin Vandersloot^{1,2,†}

¹*Institute for Gravitational Physics and Geometry,
Physics Department, The Pennsylvania State University,
University Park, PA 16802, U.S.A.*

²*Institute for Cosmology and Gravitation,
University of Portsmouth,
Portsmouth, PO1 2EG, UK*

In homogeneous and isotropic loop quantum cosmology, gravity can behave repulsively at Planckian energy densities leading to the replacement of the big bang singularity with a big bounce. Yet in any bouncing scenario it is important to include non-linear effects from anisotropies which typically grow during the collapsing phase. We investigate the dynamics of a Bianchi I anisotropic model within the framework of loop quantum cosmology. Using effective semi-classical equations of motion to study the dynamics, we show that the big bounce is still predicted with only differences in detail arising from the inclusion of anisotropies. We show that the anisotropic shear term grows during the collapsing phase, but remains finite through the bounce. Immediately following the bounce, the anisotropies decay and with the inclusion of matter with equation of state $w < +1$, the universe isotropizes in the expanding phase.

PACS numbers: 04.60.Kz, 04.60.Pp, 98.80.Qc, 03.65.Sq

I. INTRODUCTION

Recently, the investigation of loop quantum cosmology (For a review see [1]) in homogeneous and isotropic universes has indicated that the classical big-bang singularity can be replaced with a big-bounce [2, 3, 4, 5, 6]. In these scenarios gravity can be interpreted as becoming repulsive in the Planckian high energy regime, implying that our current expanding universe would have been preceded by a contracting phase. The presence of a big-bounce has been shown to be a rather generic and genuine feature of the quantum gravitational effects of loop quantum cosmology and does not require any exotic matter which violates energy conditions [7]. An exciting fact of bouncing cosmological models is that the scales measured in the cosmic microwave background (CMB) can be in causal contact if the current expanding phase is preceded by a contracting one, thus opening the possibility for a replacement of the standard inflationary scenario.

In order to more fully develop this scenario, one must go beyond the assumption of homogeneity and isotropy. It is both the inhomogeneities and anisotropies that are expected to grow in a collapsing phase and thus a proper accounting of these fluctuations is required. One particular question that immediately arises is whether the presence of the bounce is stable under the inclusion of inhomogeneities and anisotropies. A proper description of the inhomogeneous perturbations and anisotropies would then provide an answer to the question of whether a suit-

able alternative to inflation can be constructed, and/or what possible cosmological signatures may result.

In this paper we do not seek to answer all these questions as work on including inhomogeneities in loop quantum cosmology is in its infancy (initial progress can be found in [8, 9, 10, 11]). Instead, we will focus on the behavior of anisotropies, studying the dynamics of the anisotropic Bianchi I model in the framework of loop quantum cosmology. In the classical Bianchi I universe sourced with matter with zero anisotropic stress, the anisotropic shear term behaves as an effective matter component with energy density that scales as a^{-6} in the Friedmann equation with a being the mean scale factor. Thus for matter with equation of state $w < +1$, the anisotropies will dominate the collapsing phase as the singularity is approached. If the current expanding phase of the universe was preceded by a collapsing phase, the inclusion of anisotropies can be expected to play a significant result near the bounce.

The loop quantization of the anisotropic Bianchi I model was initially studied in [12] and more recently in [13]. In this paper, we will study the dynamics of the model at the level of effective classical equations of motion that incorporate quantum effects arising from the loop quantum Einstein equations. At the level of the effective equations we study, we show that the big-bounce is indeed robust under the inclusion of non-linear anisotropies. We will show that the anisotropic shear remains finite through the bounce and that if matter with equation of state $w < +1$ is included, the universe isotropizes in the expanding phase. The results represent evidence that the bouncing scenario of loop quantum cosmology is robust when the assumptions of homogeneity and isotropy are relaxed and gives hope that the same can be said when inhomogeneous perturbations are properly

*Electronic address: chiou@gravity.psu.edu

†Electronic address: Kevin.Vandersloot@port.ac.uk

included in the theory.

II. CLASSICAL DYNAMICS

We start with the classical setup for the Bianchi I model. Loop quantum cosmology is based on a Hamiltonian formulation and thus we will define the Hamiltonian for the gravitational plus matter degrees of freedom. Hamilton's equations of motion then are equivalent to Einstein's equations for the model considered. Since the starting point of the quantization is the Hamiltonian, it is there that we will incorporate the quantum effects in a modified effective Hamiltonian to be introduced in the next section.

Starting with the dynamical variables that comprise the classical phase space, we have three triad variables \tilde{p}_I and three connection variables \tilde{c}_I with $I = 1, 2, 3$. The classical metric given in terms of the directional scale factors a_I is

$$ds^2 = -N^2 dt^2 + a_1^2 dx^2 + a_2^2 dy^2 + a_3^2 dz^2 \quad (1)$$

with N representing the lapse which is a freely specified function representing the freedom to redefine the time variable, and the coordinates x, y, z are all valued on the entire real line (we are not considering a compactified model). The triad variables are directly related to the scale factors as

$$|\tilde{p}_1| = a_2 a_3, \quad |\tilde{p}_2| = a_1 a_3, \quad |\tilde{p}_3| = a_1 a_2. \quad (2)$$

Thus the triad variables encode information about the spatial geometry. The connection \tilde{c}_I will encode information about the curvature (essentially time derivatives of the scale factors) as will be evident once Hamilton's equations are solved.

In the Hamiltonian framework, the classical equations of motion are derived from a Hamiltonian obtained by inserting the homogeneous phase space variables into the Hamiltonian of general relativity making it a functional of \tilde{p}_I and \tilde{c}_I in this case. However, a non-triviality arises from the spatial integrations in the Hamiltonian. Because of homogeneity, these integrations diverge since we are considering the non-compact Bianchi I model. To overcome this, the spatial integrations can be restricted to a finite sized fiducial cell with fiducial volume $V_0 = \int d^3x$. We can use the fiducial cell to define untilded variables p_I, c_I as

$$p_I = V_0^{2/3} \tilde{p}_I, \quad c_I = V_0^{1/3} \tilde{c}_I. \quad (3)$$

In the classical theory, one can freely rescale the coordinates x, y, z while leaving the physics invariant. Under this rescaling, one can show that the untilded variables p_I, c_I are invariant. Since the quantization is based on the untilded variables, the quantum theory is manifestly invariant under this coordinate rescaling. This is entirely analogous to the non-compact isotropic $k = 0$ [14] and $k = -1$ [6] models where the same procedure is used.

With the understanding that the spatial integrations in the Hamiltonian are restricted to the fiducial cell, the total Hamiltonian of the model is given by

$$\begin{aligned} \mathcal{H} &= \mathcal{H}_{\text{grav}} + \mathcal{H}_{\text{matter}} \\ &= \frac{-N}{\kappa\gamma^2\sqrt{p_1 p_2 p_3}} (c_2 p_2 c_3 p_3 + c_1 p_1 c_3 p_3 + c_1 p_1 c_2 p_2) \\ &\quad + \mathcal{H}_M. \end{aligned} \quad (4)$$

with \mathcal{H}_M being the matter Hamiltonian. Here we have $\kappa = 8\pi G$, and γ is known as the Barbero-Immirzi parameter and represents a quantum ambiguity of loop quantum gravity which is a non-negative real valued parameter. Two sets of equations of motion derived from the Hamiltonian then govern the dynamics. First, the Hamiltonian of gravity and matter is of the constrained type whereby it vanishes identically for solutions to Einstein's equations. Thus an equation of motion is given by

$$\mathcal{H} = 0. \quad (5)$$

Second, Hamilton's equations give the time evolution of any phase space variable through the Poisson bracket:

$$\dot{p}_I = \{p_I, \mathcal{H}\}, \quad \dot{c}_I = \{c_I, \mathcal{H}\}. \quad (6)$$

The Poisson structure of the gravitational variables leads to the only non-vanishing Poisson brackets

$$\{c_I, p_J\} = \kappa\gamma \delta_{IJ}. \quad (7)$$

With this, Hamilton's equations for c_I and p_I are given by

$$\dot{p}_I = -\kappa\gamma \frac{\partial \mathcal{H}}{\partial c_I}, \quad \dot{c}_I = \kappa\gamma \frac{\partial \mathcal{H}}{\partial p_I}. \quad (8)$$

To proceed further with the equations of motion, we must specify the matter Hamiltonian. We take it to be of form

$$\mathcal{H}_M = N \sqrt{p_1 p_2 p_3} \rho_M \quad (9)$$

with ρ_M being the matter energy density. In this paper, we assume that the matter has zero anisotropic stress which implies that ρ_M couples to p_I in the form

$$\rho_M(p_1, p_2, p_3) = \rho_M(p_1 p_2 p_3). \quad (10)$$

This assumption is true for scalar fields and perfect fluids which we will concentrate on in this paper. Additionally, to derive the equations of motion we must specify the form of the lapse. For simplicity of the resulting equations, let us choose a form given by

$$N = \sqrt{p_1 p_2 p_3}, \quad (11)$$

which means we are using a different time t' variable than the usual cosmic time t given by

$$dt' = (p_1 p_2 p_3)^{-1/2} dt. \quad (12)$$

Note that the choice of lapse is arbitrary and none of the physical results depend on the choice.

We now derive the classical equations of motion. The Hamiltonian with our choice of lapse is

$$\mathcal{H} = -\frac{1}{\kappa\gamma^2} (c_2c_3p_2p_3 + c_1c_3p_1p_3 + c_1c_2p_1p_2) + p_1p_2p_3\rho_M. \quad (13)$$

The first set of Hamilton's equations in (8) for the time evolution of the triad then yields for instance

$$\frac{dp_1}{dt'} = \frac{p_1}{\gamma} (c_2p_2 + c_3p_3). \quad (14)$$

Using the relations between the triad components and scale factors (2) and (3), we can solve these equations for the connection coefficients c_I to get

$$c_I = \gamma V_0^{-2/3} (a_1a_2a_3)^{-1} \frac{da_I}{dt'} \equiv \gamma V_0^{1/3} \frac{da_I}{dt}. \quad (15)$$

These relations therefore provide us with the interpretation of the connection components as containing information about the curvature, which in the the Bianchi I model is entirely encoded as the extrinsic curvature here proportional to da_I/dt .

The next set of Hamilton's equations in (8) for the time evolution of the connection yields for instance

$$\frac{dc_1}{dt'} = -\frac{c_1}{\gamma} (c_2p_2 + c_3p_3) + \kappa\gamma p_2p_3 \left(\rho_M + p_1 \frac{\partial\rho_M}{\partial p_1} \right). \quad (16)$$

Combining (14) and (16) gives a key relation

$$\frac{d}{dt'} (p_I c_I) = \kappa\gamma p_1p_2p_3 \left(\rho_M + p_I \frac{\partial\rho_M}{\partial p_I} \right). \quad (17)$$

It is here we use our assumption that the matter has zero anisotropic stress (10). This assumption implies $p_I \partial\rho_M/\partial p_I = p_J \partial\rho_M/\partial p_J$ and thus (17) yields

$$\frac{d}{dt'} (p_I c_I - p_J c_J) = 0, \quad (18)$$

which can be integrated to give

$$p_I c_I - p_J c_J = \gamma V_0 \alpha_{IJ} \quad (19)$$

with α_{IJ} being a constant anti-symmetric 3×3 matrix satisfying by construction $\alpha_{12} + \alpha_{23} + \alpha_{31} = 0$ and the factors of γ, V_0 are chosen for convenience. Written in terms of the scale factors this implies

$$H_I - H_J = \frac{\alpha_{IJ}}{a_1 a_2 a_3} \quad (20)$$

for the directional Hubble rates (in terms of cosmic time $dt = V_0 a_1 a_2 a_3 dt'$)

$$H_I \equiv \frac{\dot{a}_I}{a_I}. \quad (21)$$

Using (20) and the vanishing of the Hamiltonian, we can write down a generalized Friedmann equation. The vanishing of the Hamiltonian (13) gives in terms of the Hubble rates

$$H_1 H_2 + H_1 H_3 + H_2 H_3 = \kappa \rho_M. \quad (22)$$

Let us next define the mean scale factor a as

$$a = (a_1 a_2 a_3)^{1/3}, \quad (23)$$

from which the following relation holds

$$\frac{\dot{a}}{a} = \frac{1}{3} (H_1 + H_2 + H_3). \quad (24)$$

This relation implies

$$\left(\frac{\dot{a}}{a} \right)^2 = \frac{1}{3} (H_1 H_2 + H_1 H_3 + H_2 H_3) + \frac{1}{18} [(H_1 - H_2)^2 + (H_1 - H_3)^2 + (H_2 - H_3)^2]. \quad (25)$$

Finally, using (20) and (22), the generalized Friedmann equation becomes

$$\left(\frac{\dot{a}}{a} \right)^2 = \frac{\kappa}{3} \rho_M + \frac{\Sigma^2}{a^6}, \quad (26)$$

where Σ is given in terms of the constants of motion α_{IJ} as

$$\Sigma^2 \equiv \frac{1}{18} (\alpha_{12}^2 + \alpha_{23}^2 + \alpha_{31}^2). \quad (27)$$

The *anisotropic shear* $\sigma_{\mu\nu} \sigma^{\mu\nu}$ is related to Σ through

$$\begin{aligned} \sigma_{\mu\nu} \sigma^{\mu\nu} &\equiv \frac{1}{3} \left((H_1 - H_2)^2 + (H_2 - H_3)^2 + (H_3 - H_1)^2 \right) \\ &= \frac{6\Sigma^2}{a^6}. \end{aligned} \quad (28)$$

The equations of motion for $a(t)$ can now be determined from the generalized Friedmann equation (26). The time evolution for the directional scale factors $a_I(t)$ can then be determined from a combination of (20) and (24), once $a(t)$ is known.

Let us discuss the interpretation of the generalized Friedmann equation (26). We first recognize the isotropic matter term $\kappa\rho_M/3$ on the right hand side with the anisotropic shear term behaving as a stiff fluid with equation of state $w = +1$. The isotropic limit is achieved when $\alpha_{IJ} = 0, \Sigma = 0$ which from the relations (20) implies that the directional Hubble rates H_I are identical indicating isotropic expansion. Because the shear terms scales as a^{-6} , for typical forms of matter the early universe can be anisotropy dominated, with matter then dominating the later stages. In particular, if $w < +1$, the later stages of expansion tend to a more isotropic state, whereby the Hubble rates become identical in all directions. Oppositely, as the singularity is approached,

the universe behaves like a vacuum universe as the shear term dominates the matter term and Kasner like behavior occurs. This behavior is described in more detail in appendix A.

As an example, let us consider a dust filled ($w = 0$) Bianchi I universe with matter density $\rho_M = \tilde{A}/a^3$. The generalized Friedmann equation can be solved analytically giving

$$a(t) = \left[\frac{3\kappa\tilde{A}}{4} t^2 + 3\Sigma t \right]^{1/3}, \quad (29)$$

which gives the standard dust filled isotropic behavior at late times $a \propto t^{2/3}$ while at early times is anisotropy dominated $a \propto t^{1/3}$ and is singular at $t = 0$. The time evolution of the individual scale factors can then be determined from (20) and (24), which gives for instance

$$a_1(t) = \left(\frac{3\kappa\tilde{A}}{4} + \frac{3\Sigma}{t} \right)^{\frac{-\alpha_{12} + \alpha_{31}}{9\Sigma}} a(t). \quad (30)$$

Let us consider the situation where initially a_1 is contracting with the other two directions expanding. In this case we have $\alpha_{12} < 0$ and $\alpha_{31} > 0$. It is easy to see from (30), that at late times $a_1(t)$ behaves as $a_1(t) \approx a(t) \propto t^{2/3}$ and thus is *expanding* in accordance with the isotropic behavior. At early times, however, it is not too difficult to show that (30) implies contraction ($\dot{a}_1 < 0$) and thus the scale factor bounces at some finite time and eventually the universe isotropizes to a matter dominated phase. Therefore with matter with equation of state $w < +1$, the universe can initially be in a Kasner like epoch with one direction contracting and the other two expanding; eventually, however, such a universe will isotropize giving expansion in all three directions.

Thus, at the classical level the anisotropies are expected to play an important role as the singularity is approached. In the isotropic setting of loop quantum cosmology, the bouncing scenario has been well described in terms of an effective Friedmann equation of the form [4]

$$H^2 = \frac{\kappa}{3} \rho_M \left(1 - \frac{\rho_M}{\rho_{\text{crit}}} \right) \quad (31)$$

with $\rho_{\text{crit}} \approx .82\rho_{\text{Pl}}$ being a critical energy density of Planckian order. When the matter density reaches the critical density, $H = 0$ indicating a bounce. Because the bounce occurs in the high energy regime near the classical singularity, it is important to include the effects of the anisotropies. In the next section we will answer the question as to what role the anisotropies play in the bouncing scenario.

III. EFFECTIVE LOOP QUANTUM DYNAMICS

As we have stated, the quantum modifications due to loop quantum cosmology that we study exhibit themselves in the form of a modified effective Hamiltonian.

Since we study effective *classical* equations of motion, we are by definition ignoring certain quantum degrees of freedom. Properly speaking, in the quantum theory, dynamics is understood through expectation values of observables calculated from semi-classical wave packets. Thus additional effects which we do not study can arise from features of the semi-classical state such as the spread and so forth. The effective quantum modifications we study to first order are insensitive to the features of the semi-classical wavefunction and are expected to be valid provided the wavepacket remains sharply peaked though the evolution. That this is a good approximation has been verified in the isotropic models of LQC sourced with a massless scalar field[4, 5, 6], where the quantum dynamics have been extensively developed and understood. Note that the effective equations we consider are somewhat heuristically motivated and more systematic approaches to deriving effective equations have been considered [15], but ultimately proper justification of any effective scheme requires the study of the quantum dynamics.

The main quantum effect arises from the fact that in LQC, the connection variables c_I do not have direct quantum analogues and are replaced by holonomies (roughly exponentials of the connection). This manifests itself in the effective Hamiltonian by replacing the classical c_I terms with sine functions

$$c_I \longrightarrow \frac{\sin(\bar{\mu}_I c_I)}{\bar{\mu}_I}, \quad (32)$$

where $\bar{\mu}_I$ are real valued functions of the triad coefficients p_I which are a measure of the discreteness in the quantum theory. Classical behavior is expected in the limit when $\bar{\mu}_I c_I \ll 1$ whence $\sin(\bar{\mu}_I c_I)/\bar{\mu}_I \approx c_I$.

In the original construction of LQC, the $\bar{\mu}_I$ were taken to be constants (referred to as μ_0)[12]; however it has been shown that in the isotropic case this can lead to the wrong semi-classical limit[4]. In the isotropic case it has been argued that $\bar{\mu}$ should not be a constant, but should scale as $\bar{\mu} \propto 1/\sqrt{p}$ which has been shown to have a nice semi-classical limit[4]. Extending this scheme to the Bianchi I model is slightly more ambiguous as several possibilities exist. We choose in this paper to focus on the scheme proposed in [13] where $\bar{\mu}_I$ are given by

$$\bar{\mu}_I = \sqrt{\frac{\Delta}{p_I}}, \quad (33)$$

where $\Delta = \frac{\sqrt{3}}{2}(4\pi\gamma\ell_{\text{Pl}}^2)$ is the *area gap* in the full theory of LQC and $\ell_{\text{Pl}} \equiv \sqrt{G\hbar}$ is the Planck length. An alternative scheme would be to have $\bar{\mu}_I \propto 1/a_I$ which we will briefly discuss in Appendix C. However the main physical results we will describe do not depend sensitively on either of the scheme; only the quantitative results would change. Better input from the full theory might provide justification for either scheme. One advantage of the scheme (33) is that it is more amenable to the study

of dynamics with semi-classical states in the quantum theory, as the resulting difference equation is much simpler. This would allow for the test of the validity of the results presented here, by examining semi-classical state behavior in the quantum theory.

Additional modifications due to loop quantum cosmology have been studied extensively in the isotropic setting and pertain to operator eigenvalues of inverse p_I factors that would appear in the matter part of the effective Hamiltonian. In the isotropic setting this amounts to replacing factors of $p^{-3/2}$ in the matter Hamiltonian by an operator eigenvalue function $d_j(p)$ which is bounded and vanishes at $p = 0$ corresponding to the classical singularity.¹ Additionally an ambiguity parameter j appears such that larger values amplify the d_j effects. In this paper we will for simplicity ignore these effects in accordance with arguments that j should take its smallest value [16, 18], as well as questions as to the ambiguous nature of the critical scale at which the corrections are appreciable. Further discussion can be found in [4, 5, 6, 19]. Our results presented here will remain valid as long as the critical scale remains below the scale at which the bounce occurs. In lieu of this, in our analysis the matter energy density ρ_M appearing in the effective Hamiltonian (34) will not contain factors of d_j and will assume the classical form.

With these caveats in mind, the effective Hamiltonian with lapse $N = \sqrt{p_1 p_2 p_3}$ is given by

$$\mathcal{H}_{\text{eff}} = -\frac{1}{\kappa\gamma^2} \left\{ \frac{\sin(\bar{\mu}_2 c_2) \sin(\bar{\mu}_3 c_3)}{\bar{\mu}_2 \bar{\mu}_3} p_2 p_3 + \text{cyclic terms} \right\} + p_1 p_2 p_3 \rho_M \quad (34)$$

and it becomes easy to see that in the limit of small $\bar{\mu}_I c_I$, the classical Hamiltonian (13) is recovered.

Hamilton's equations proceed in the same fashion as the classical setup. The equations for dp_I/dt' and dc_I/dt' give for instance

$$\frac{dp_1}{dt'} = \frac{p_1 \cos(\bar{\mu}_1 c_1)}{\gamma} \left\{ p_2 \frac{\sin(\bar{\mu}_2 c_2)}{\bar{\mu}_2} + p_3 \frac{\sin(\bar{\mu}_3 c_3)}{\bar{\mu}_3} \right\} \quad (35)$$

and

$$\begin{aligned} \frac{dc_1}{dt'} &= -\frac{1}{\gamma} \left(\frac{3 \sin(\bar{\mu}_1 c_1)}{2 \bar{\mu}_1} - \frac{c_1 \cos(\bar{\mu}_1 c_1)}{2} \right) \\ &\quad \times \left\{ p_2 \frac{\sin(\bar{\mu}_2 c_2)}{\bar{\mu}_2} + p_3 \frac{\sin(\bar{\mu}_3 c_3)}{\bar{\mu}_3} \right\} \\ &\quad + \kappa\gamma p_2 p_3 \left(\rho_M + p_1 \frac{\partial \rho_M}{\partial p_1} \right). \end{aligned} \quad (36)$$

Hamilton's equations are now more complicated since the discreteness parameters $\bar{\mu}_I$ depend on p_I , but let us define $\mathcal{G}_I(t')$ as

$$\mathcal{G}_I(t') := p_I \frac{\sin(\bar{\mu}_I c_I)}{\bar{\mu}_I}, \quad (37)$$

which can be shown to satisfy

$$\frac{d\mathcal{G}_I}{dt'} = \kappa\gamma \cos(\bar{\mu}_I c_I) p_1 p_2 p_3 \left(\rho_M + p_I \frac{\partial \rho_M}{\partial p_I} \right). \quad (38)$$

The vanishing of the Hamiltonian gives

$$\kappa\gamma^2 p_1 p_2 p_3 \rho_M = \mathcal{G}_1 \mathcal{G}_2 + \mathcal{G}_1 \mathcal{G}_3 + \mathcal{G}_2 \mathcal{G}_3. \quad (39)$$

Note that the classical limit is attained by $\bar{\mu}_I c_I \rightarrow 0$, where we have $\sin(\bar{\mu}_I c_I)/\bar{\mu}_I \rightarrow c_I$, $\cos(\bar{\mu}_I c_I) \rightarrow 1$ and therefore (35), (36), (38) reduce to their classical counterparts (14), (16), (17).

At this stage, the equations are too complicated to solve analytically as was possible classically. To get a handle for the evolution, we can consider as an example, the case of a massless scalar field with equation of state $w = +1$ whereby the equations simplify considerably. With a massless scalar field, we have

$$\rho_M = \frac{P_\phi^2}{2p_1 p_2 p_3}, \quad (40)$$

where the momentum P_ϕ^2 is a constant of motion. Therefore, the term $\rho_M + p_I \frac{\partial \rho_M}{\partial p_I}$ in (38) vanishes identically. From this we find that \mathcal{G}_I are all constants in time. Equation (37) then implies that the triad components are all bounded as

$$p_I \geq \left(|\mathcal{G}_I| \sqrt{\Delta} \right)^{2/3}, \quad (41)$$

implying that the classical singularity is never approached. One can show from the equations of motion, that $\dot{p}_I > 0$ when $p_I = (|\mathcal{G}_I| \sqrt{\Delta})^{2/3}$ implying that the individual triad components p_I bounce and hence the whole universe must bounce. With this bound one can show that no curvature invariants blow up, and the dynamics is non-singular.² Note that this analysis holds for the vacuum case if $P_\phi = 0$. Therefore a bounce would occur generically for the vacuum case also.

Thus, at least with a massless scalar field, the bounce is robust under the inclusion of anisotropies. Next we can monitor the behavior of the anisotropic shear term through the bounce for this example. If we look at the

¹ Similar inverse triad effects appear in the gravitational Hamiltonian leading to a function $s_j(p)$ [16]. These corrections have been typically been ignored, but see [17] for work on some cosmological implications.

² There is a special case when one of the \mathcal{G}_I vanishes whence p_I is not constrained above a minimum value. However, this is the special case when p_I is a constant which can be seen from (35). Therefore the specific triad component does not become zero and the evolution remains non-singular.

shear parameter Σ we showed that classically it remains constant throughout the evolution. With the loop quantum modifications we can monitor its behavior by using its definition

$$\Sigma^2 := \frac{a^6}{18} \left((H_1 - H_2)^2 + (H_2 - H_3)^2 + (H_3 - H_1)^2 \right), \quad (42)$$

which in the classical case was a constant because of equation (21). In the LQC case, let us assume we start with a nearly classical contracting universe with each $\bar{\mu}_I c_I \ll 1$. In this limit from (37) we find

$$\mathcal{G}_I \approx p_I c_I. \quad (43)$$

Since \mathcal{G}_I are constant for the massless scalar field, we can identify them with the classical constants α_{IJ} from (19) as $\mathcal{G}_I - \mathcal{G}_J = \gamma V_0 \alpha_{IJ}$. The shear factor Σ is then given initially as

$$\Sigma^2(\text{pre bounce}) \approx \frac{1}{18\gamma V_0} \left((\mathcal{G}_1 - \mathcal{G}_2)^2 + \text{cyclic terms} \right). \quad (44)$$

After the bounce, the constancy of \mathcal{G}_I and equation (37) imply that $\bar{\mu}_I c_I$ become small as p_I grow and hence classical behavior is recovered at late times. We can apply the same argument to conclude that the late time behavior of Σ approaches the pre-bounce value in terms of the same constants \mathcal{G}_I :

$$\Sigma^2(\text{post bounce}) = \Sigma^2(\text{pre bounce}) \quad (45)$$

and hence the shear factor Σ is conserved before and after the bounce. Using equations (35) and (37), it is not too difficult to show that the shear term remains finite through the bounce indicating that the anisotropies do not blow up.

The similar conclusions can be obtained for the generic cases with the inclusion of arbitrary matter with $w < +1$. The details of the effective loop quantum dynamics with generic perfect fluids are investigated in Appendix B. The detailed analysis shows that individual p_I in different directions can bounce at slightly different moments. Moreover, there is competition between the matter energy density ρ_M and the *directional density* ϱ_I (defined in (B10), which is associated with the classical anisotropic shear) to be dominant when the quantum corrections start to become significant. As a result, depending on how energetic the matter content is (compared to the degree of anisotropies), the bounce can take place either in the ‘‘Kasner phase’’ or in the ‘‘isotropized phase’’ (or in the ‘‘transition phase’’ in between). If quantum corrections take effect in the isotropized phase, the bounce happens around the moment when ρ_M approaches $.82\rho_{P1}$, giving similar results as in the isotropic model. On the other hand, if the bounce occurs in the Kasner phase, the individual triad components bounce when ϱ_I approach $.86\rho_{P1}$.

In the case that the big bounce occurs in the isotropized phase, the Kasner fashion of the classical solution is smeared by the quantum effect and thus the

information of anisotropies is blurred. Therefore, on the other side of the bounce, the classical anisotropic shear is changed. This explains why $\Sigma^2(\text{post bounce}) \neq \Sigma^2(\text{pre bounce})$ in general. Only in the case when the big bounce takes place in the Kasner phase do we have $\Sigma^2(\text{post bounce}) \approx \Sigma^2(\text{pre bounce})$.³

In the next section we explicitly show the results mentioned here by numerically solving the equations of motion.

IV. NUMERICAL RESULTS

Owing to the complexity of the effective equations of motion, we can not go further in the analytical analysis for more general forms of matter. In this section we will present some numerical simulations of the equations of motion by including other forms of matter. In particular we will focus on whether a bounce occurs for an initially contracting universe and how the shear term Σ behaves through the bounce. Additionally we will show that the universe isotropizes after the bounce with the inclusion of $w < +1$ matter.

The differential equations for the time evolution of $p_I(t')$ and $c_I(t')$ are given in (35) and (36). Numerically we solve the equations given a lapse N equal to one and plot as a function of cosmic time t . The initial conditions are chosen consisting of a collapsing semi-classical universe such that $\dot{a} < 0$ and $\bar{\mu}_I c_I \ll 1$. The shear term Σ is monitored using the classical formula (28).

The first example we consider is the vacuum case. The analysis can be understood analytically as a special case of the massless scalar field studied in the previous section. The same analysis holds when $P_\phi = 0$ which gives the vacuum case. Therefore, for a vacuum case a bounce is generic and the shear term Σ^2 is conserved before and after the bounce.

The mean scale factor $a(t)$, directional scale factors $a_I(t)$, and shear term $\Sigma^2(t)$ are plotted in Figures 1 and 2 respectively, for a representative numerical simulation consisting of an initially contracting universe which in the vacuum Kasner case requires two contracting directions and one expanding. After the bounce, the universe consists of a Kasner like expanding phase with growth in two directions and contraction in the other. Throughout the evolution, the shear term remains finite with the behavior during the bounce showing no obvious pattern (from numerical simulations, the exact behavior can depend on initial conditions and choice of matter). However, it is clear that the post-bounce value tends to the pre-bounce

³ In the cases of vacuum and with only massless scalar field, the classical solution remains in Kasner phase throughout the evolution (the universe is not isotropized by matter). Thus, quantum corrections always take effect in the Kasner phase and this is why we have $\Sigma^2(\text{post bounce}) = \Sigma^2(\text{pre bounce})$ exactly for these two special cases.

value as shown by the analytical arguments of the previous section.

The inclusion of a massless scalar field does not change the results of the vacuum case significantly. With matter, the initial contracting phase can be either one where all directions contract, or a Kasner like contraction as in the vacuum case. In Figures 3 and 4, the scale factors and shear term are plotted for the case where all three directions initially are contracting. Again, the shear term is finite through the evolution and the post-bounce value approaches the pre-bounce value, as expected from the analytical analysis.

As an example of the inclusion of other forms of matter, we consider a radiation ($w = 1/3$) field with energy density

$$\rho_M = \frac{\tilde{A}}{a^4} \quad (46)$$

with \tilde{A} some constant. The numerical behavior of the scale factor appears in Figure 5, where again the bounce occurs. Various initial conditions were examined and in all cases the bounce occurred providing evidence that it is a general feature of the effective Hamiltonian we study in this paper. In contrast to the massless scalar field case, the shear term is not conserved after the bounce. This is shown in Figure 6, and for the particular initial conditions chosen, actually decreases in the post-bounce regime. It must be stated that the decrease is not a generic feature and is sensitive to the initial conditions. However, as in the previous cases, the shear term is finite through the entire evolution.

Since the equation of state for the radiation field $w = 1/3 < +1$, the post-bounce regime leads to an isotropization of the universe. This is borne out in the numerical simulations in Figure 7. There are plotted ratios of the directional Hubble ratios. The ratios approach unity in the post-bounce epoch indicating identical expansion rates in the three directions.

V. DISCUSSION

Let us restate the main results presented. We have considered the anisotropic Bianchi I model with loop quantum corrections to the classical equations of motion. We have shown that a bounce occurs under rather generic conditions in a collapsing universe. The anisotropic shear term Σ^2/a^6 , which classically grows during collapse and blows up at the singularity, remains finite through the bounce. After the bounce, the universe behaves more and more classically and can isotropize at later times. This is thus evidence that the bouncing scenario of the isotropic models of loop quantum cosmology is robust when the symmetries of the isotropic model are relaxed.

We must reiterate the caveats that has gone into this analysis. First, we have used entirely the effective classical equations of motion determined from the effective

Hamiltonian (34). This effective Hamiltonian is motivated from the construction of the quantum Hamiltonian operator in a somewhat heuristic fashion. In principle, however, there can be additional modifications arising from the quantum theory. To properly justify the analysis here, more work is required to analyze the quantum dynamics by constructing semi-classical states and evolving them with the quantum difference equation. The accuracy of the effective equations of motion has been established in the isotropic case with a massless scalar field, and thus we expect that they should give an accurate representation of the dominant corrections arising in the quantum dynamics.

In addition, we have ignored the inverse triad effects arising in loop quantum cosmology. One might ask if we do include these effects, does the bounce picture still hold. Yet, we can answer this by noting that the inverse triad modifications tend to suppress the matter energy density. Thus if the suppression is large, the universe behaves more like a vacuum Bianchi I model. Our analysis indicates that the bounce still occurs in this case. Therefore, the inverse triad effects are not expected to remove the bounce, and only change the quantitative behavior.

We have not considered in this paper additional anisotropic Bianchi models. It would be interesting to extend the analysis to these models. In particular the results in principle could be extended to the Bianchi IX model. An interesting question would be whether the quantum effects tame the classical chaos in the model and again whether a bounce is predicted. Additionally, since the Bianchi IX model has been conjectured to be of relevance to singularities in general, the analysis may provide hints as to what role loop quantum effects play with regards to general singularities.

Acknowledgments

The authors would like to thank Abhay Ashtekar, Martin Bojowald, Golam Hossain, Roy Maartens, Tomasz Pawłowski and Parampreet Singh for useful discussions. This work was supported in part by the NSF grant PHY-0456913, the Eberly research funds of Penn State, and the Marie Curie grant MIF1-CT-2006-022239.

APPENDIX A: DETAILS OF THE CLASSICAL SOLUTIONS

In this appendix we discuss in more detail the solutions to the classical equations of motion. We show explicitly how the universe near the singularity is dominated by Kasner like dynamics and how the universe can isotropize far away from the singularity for matter with $w < 1$.

Let us start with the relation (18), which, in addition to (19), implies

$$p_I c_I = \kappa \gamma \hbar [\mathcal{K}_I + f(t')] \quad (A1)$$

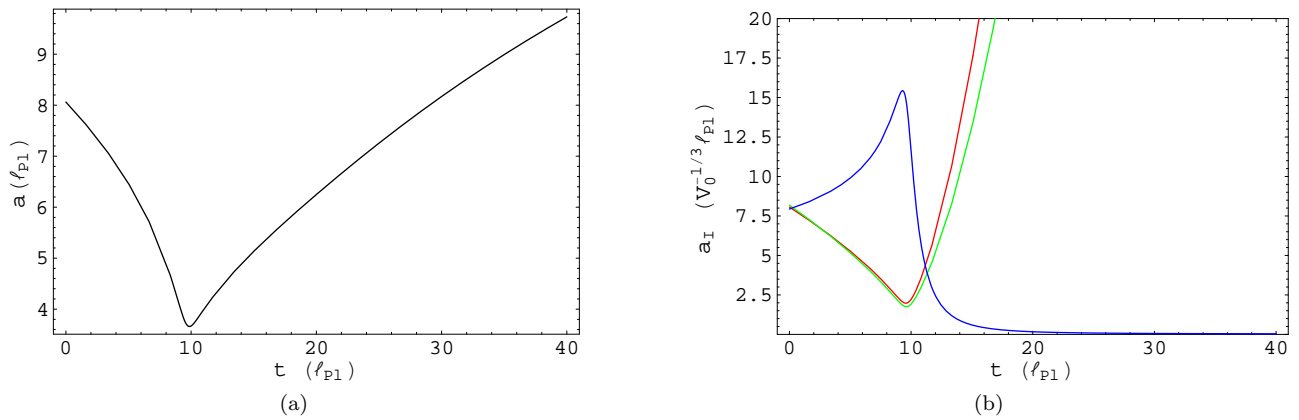


FIG. 1: Mean scale factor $a(t)$ and directional scale factors $a_I(t)$ for vacuum $\rho_M = 0$ case. The initial conditions are chosen corresponding to an initially contracting universe.

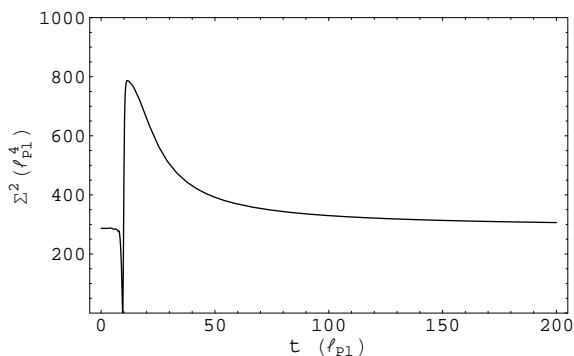


FIG. 2: Shear term for vacuum case. Classically, the value is a constant, though quantum mechanically it is not constant near the bounce. The post-bounce value approaches the pre-bounce value, and nowhere does it blow up.

with the dimensionless constants of motion \mathcal{K}_I . Note that

$$\kappa\hbar(\mathcal{K}_I - \mathcal{K}_J) = V_0\alpha_{IJ}. \quad (\text{A2})$$

We assume that the matter density is in the form

$$\rho_M = A(p_1 p_2 p_3)^{-(1+w)/2} \quad (\text{A3})$$

with A a constant and w the state parameter.

The Hamiltonian constraint $\mathcal{H} = 0$ with \mathcal{H} given by (13) then yields

$$3f(t')^2 + 2(\mathcal{K}_1 + \mathcal{K}_2 + \mathcal{K}_3)f(t') + \mathcal{K}_2\mathcal{K}_3 + \mathcal{K}_1\mathcal{K}_3 + \mathcal{K}_1\mathcal{K}_2 = (\kappa\hbar^2)^{-1}A(p_1 p_2 p_3)^{\frac{1-w}{2}}, \quad (\text{A4})$$

which gives the time-independent part:⁴

$$\mathcal{K}_2\mathcal{K}_3 + \mathcal{K}_1\mathcal{K}_3 + \mathcal{K}_1\mathcal{K}_2 = 0 \quad (\text{A5})$$

⁴ We can always absorb an arbitrary constant to $f(t')$ and thus

and the time-dependent part:

$$f(t') = -\frac{\mathcal{K}_1 + \mathcal{K}_2 + \mathcal{K}_3}{3} \pm \frac{1}{3} \left[(\mathcal{K}_1 + \mathcal{K}_2 + \mathcal{K}_3)^2 + \frac{3A(p_1 p_2 p_3)^{\frac{1-w}{2}}}{\kappa\hbar^2} \right]^{1/2}. \quad (\text{A6})$$

We can scale the constants $\mathcal{K}_I = \mathcal{K}\kappa_I$ such that (A5) gives

$$\kappa_1 + \kappa_2 + \kappa_3 = 1, \quad \kappa_1^2 + \kappa_2^2 + \kappa_3^2 = 1, \quad (\text{A7})$$

which coincide with the ‘‘Kasner condition’’ satisfied by the parameters κ_I used for the vacuum Bianchi I solutions (Kasner solutions). [For the Kasner solutions, apart from the trivial solution (Minkowski spacetime), two of κ_I must be positive while the other negative, giving the universe expanding in two direction and contracting in the other (or the other way around if $\mathcal{K} < 0$).] Furthermore, note that the opposite choice of the sign \pm in (A6) amounts to the changes: $f(t') \rightarrow -f(t')$ and $\mathcal{K}_I \rightarrow -\mathcal{K}_I$ simultaneously, which correspond to the time reversal. Therefore, without losing generality, we can stick with positive sign for $A > 0$; for $A < 0$, on the other hand, \pm flips sign when the part inside the square bracket of (A6) approaches zero.⁵ We assume $A > 0$ in this paper for ordinary matter with positive energy. With (A1) and

change the dichotomy between the time-independent and time-dependent parts. However, we pick the particular choice as in (A5) and (A6) in order to relate \mathcal{K}_I to the standard parameters used in the Kasner solutions.

⁵ For $A < 0$, \pm changes signs and thus the solutions of (A8) may encounter recollapse. This is the case for the model with negative cosmological constant $\Lambda < 0$.

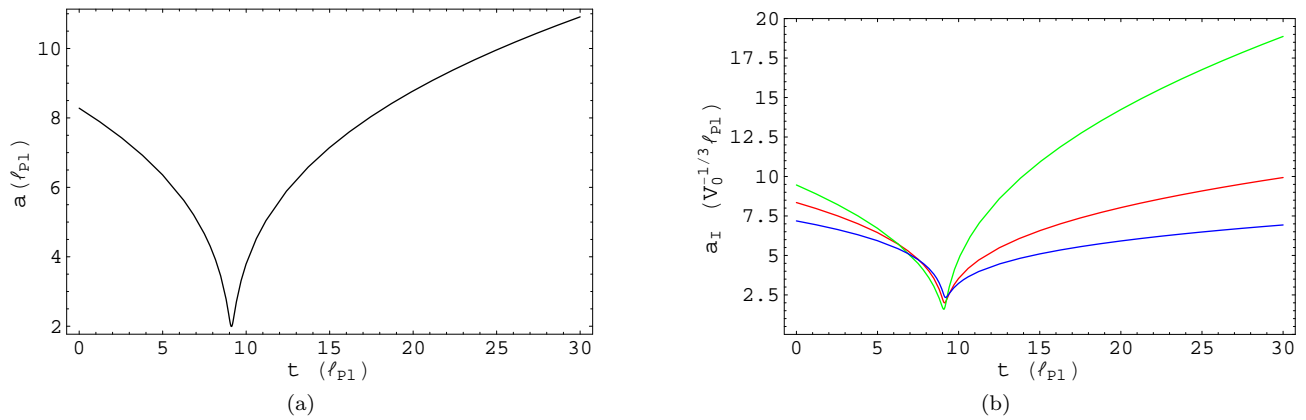


FIG. 3: Mean scale factor $a(t)$ and directional scale factors $a_I(t)$ for a massless scalar field with momentum $P_\phi = 10l_p^2$. Initially, all directions are contracting and a bounce occurs leading to expansion in all directions.

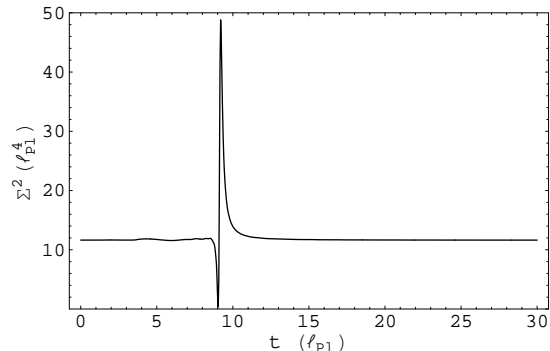


FIG. 4: Shear term for massless scalar field. As in the vacuum case, the pre-bounce value is conserved after the bounce.

(A6), the equation of motion (14) gives

$$\begin{aligned} \frac{1}{p_1} \frac{dp_1}{dt'} &= \frac{1}{\gamma} (c_2 p_2 + c_3 p_3) = \kappa \hbar [\mathcal{K}_2 + \mathcal{K}_3 + 2f(t')] \\ &= \kappa \hbar \left\{ \frac{\mathcal{K}_2 + \mathcal{K}_3 - 2\mathcal{K}_1}{3} \right. \\ &\quad \left. + \frac{2}{3} \left[(\mathcal{K}_1 + \mathcal{K}_2 + \mathcal{K}_3)^2 + \frac{3A (p_1 p_2 p_3)^{\frac{1-w}{2}}}{\kappa \hbar^2} \right]^{1/2} \right\}. \end{aligned} \quad (\text{A8})$$

For $w < 1$, the second term in the square bracket of (A8) is negligible when the solution approaches the big bang singularity; on the opposite side, it becomes dominant in the large universe limit.⁶ Therefore, in the vicini-

ty of the singularity, (A8) is approximated as

$$\frac{1}{p_1} \frac{dp_1}{dt'} \approx \kappa \hbar (\mathcal{K}_2 + \mathcal{K}_3), \quad (\text{A9})$$

yielding the solutions very close to Kasner solutions, which are highly anisotropic. On the other hand, in the large universe limit, (A8) have the asymptotic behavior

$$\frac{1}{p_1} \frac{dp_1}{dt'} \equiv \frac{(p_1 p_2 p_3)^{1/2}}{p_1} \frac{dp_1}{dt} \approx 2\sqrt{\frac{\kappa A}{3}} (p_1 p_2 p_3)^{\frac{1-w}{4}}, \quad (\text{A10})$$

giving the asymptotic solution

$$p_I(t) \propto \begin{cases} t^{\frac{4}{3(1+w)}} & w \neq -1, \\ e^{2t\sqrt{\frac{\kappa A}{3}}} & w = -1. \end{cases} \quad (\text{A11})$$

As the universe approaches the asymptotic region, the three directions are all expanding with the same rate; that is, with the inclusion of matter with equation of state $w < 1$, the universe isotropizes in the expanding phase. When the contribution from matter sector is negligible and the evolution is essentially the same as the Kasner solution as given by (A9), we call it ‘‘Kasner phase’’. On the opposite, when the matter sector dominates and the universe is isotropized as given by (A10), we call it ‘‘isotropized phase’’. The situation in between is called ‘‘transition phase’’.

As anisotropy is concerned, we study the Hubble ratios, which give the asymptotic behaviors:

$$\frac{H_I}{H_J} \equiv \frac{\dot{a}_I/a_I}{\dot{a}_J/a_J} \approx \begin{cases} \kappa_I/\kappa_J & \text{for } a \rightarrow 0, \\ 1 & \text{for } a \rightarrow \infty, \end{cases} \quad (\text{A12})$$

which are implied by equations (A9) and (A10). These ratios approach unity in the isotropized phase and approach fixed constants in the Kasner phase.⁷

⁶ For $w = 1$, the second term becomes constant and so does $f(t')$; as a result, the solutions have qualitatively different features. This is the case with massless scalar field. In particular, the scalar field can be treated as ‘‘internal time’’ and the Kasner condition (A7) is modified such that ‘‘Kasner-unlike’’ solutions (namely, expanding/contracting in *all* three directions) are also

allowed [13]; plus, the anisotropy persists in the expanding phase if no other matter content is included.

⁷ Note that, however, in the special case of vacuum ($A=0$; i.e Kas-

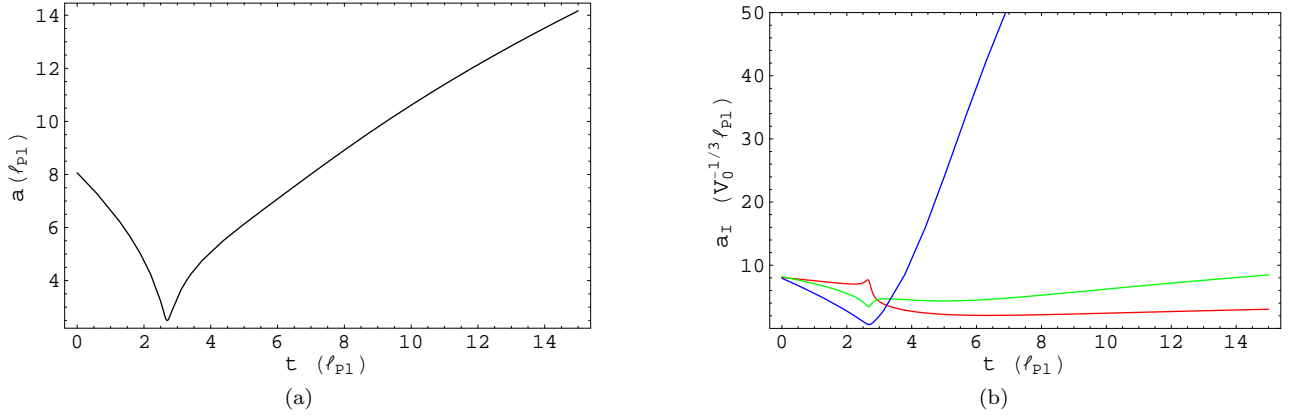


FIG. 5: Mean scale factor $a(t)$ and directional scale factors $a_I(t)$ for radiation.

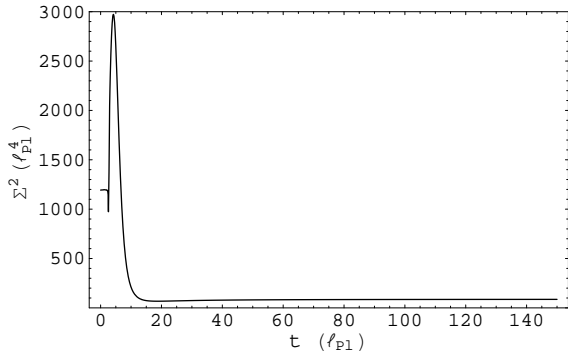


FIG. 6: Shear term for radiation. The post-bounce value does not equal the pre-bounce values although the value is finite through the entire evolution.

APPENDIX B: DETAILS OF THE EFFECTIVE LOOP QUANTUM SOLUTIONS

In order to affirm the assertions in Section III for the generic cases with arbitrary matter, this section deals with the detailed analysis for the effective loop quantum solutions. The effective dynamics with quantum corrections is governed by (35), (36) and (39), which are complicated to solve analytically for the generic case. However, we can still study two extreme cases: $a \rightarrow \infty$ and $a \rightarrow 0$.

In the limit $a \rightarrow \infty$, if $\bar{\mu}_{IC_I} \rightarrow 0$, the Hamilton's equations plus the Hamiltonian constraint simply reduce to their classical counterparts and the effective solutions are virtually the same as the classical one. We do not know *a priori* whether $\bar{\mu}_{IC_I} \rightarrow 0$ for large a and whether the quantum effect does not spoil the semi-classicality. But if the classical solutions without quantum corrections leads

ner model) or of scalar matter ($w = 1$), the Hubble ratios H_I/H_I are constant throughout the entire evolution. The classical solution does not isotropize and remains in the Kasner phase.

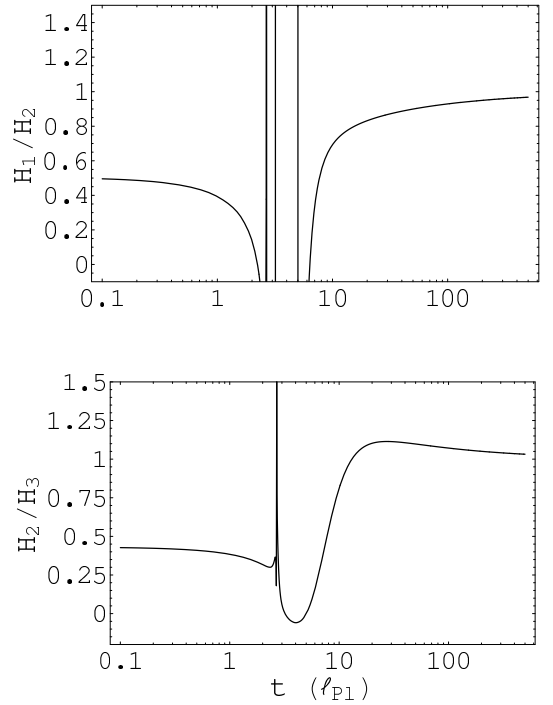


FIG. 7: Ratios of directional Hubble rates for radiation. At late times, the ratios approach unitary indicative of equal expansion rates in all directions as the universe isotropizes.

to small value of $\bar{\mu}_{IC_I}$ for large universe, we can conclude that the effective dynamics admits the solutions with semi-classicality for large a . To check this, consider the classical solutions, which have

$$\begin{aligned} p_{IC_I} &= \kappa\gamma\hbar[\mathcal{K}_I + f(t')] \approx \kappa\gamma\hbar f(t') \\ &\approx \gamma\sqrt{\frac{\kappa A}{3\hbar}} (p_1 p_2 p_3)^{\frac{1-w}{4}} \end{aligned} \quad (\text{B1})$$

for $a \rightarrow \infty$ by (A1). We then have, by (A11),

$$c_I \propto a^{-\frac{(1+3w)}{2}}, \quad \bar{\mu}_{IC_I} \propto a^{-\frac{3(1+w)}{2}}. \quad (\text{B2})$$

This shows that the quantity $\bar{\mu}_I c_I$ of classical solutions is decreasing to zero in the large universe limit for $w > -1$. Therefore, for $-1 < w < 1$, at large universe, the semi-classicality can be retained and the loop quantum corrections are indeed negligible for those solutions which are semi-classical at late times. The evolution simply follows the classical trajectory for the large universe.⁸

Now, let us study the other extreme as the universe approaches the classical singularity ($a \rightarrow 0$). In the backward evolution, before the singularity is reached, the quantum corrections will take effect and the big bounce is expected to take place. Therefore, at some point, $\cos(\bar{\mu}_I c_I)$ vanishes and flips sign. Assuming that $\cos(\bar{\mu}_I c_I)$ in different directions flip sign at only slightly different moments, we then have $\cos(\bar{\mu}_I c_I) \approx \cos(\bar{\mu}_J c_J)$ ($\rightarrow 0$) in the vicinity of the big bounce. With this approximation, close to the epoch of the big bounce, (38) yields⁹

$$\begin{aligned} & \frac{d}{dt'} (\mathcal{G}_I - \mathcal{G}_J) \\ &= \frac{1-w}{2} \kappa \gamma [\cos(\bar{\mu}_I c_I) - \cos(\bar{\mu}_J c_J)] (p_1 p_2 p_3)^{\frac{1-w}{2}} \approx 0. \end{aligned} \quad (\text{B3})$$

Thereby, we can write

$$\mathcal{G}_I \equiv p_I \frac{\sin(\bar{\mu}_I c_I)}{\bar{\mu}_I} \approx \kappa \gamma \hbar [\mathcal{K}_I + f(t')] \quad (\text{B4})$$

in accordance with the classical counterpart (A1); consequently the Hamiltonian constraint (39) gives the same $f(t')$ as given by (A6). To proceed further, in the following, we consider three cases separately: quantum corrections take effect (i) in the Kasner phase; (ii) in the isotropized phase; and (iii) in the transition phase.

In Case (i), the first term in the square bracket dominates over the second term in (A6); thereby,

$$\begin{aligned} f(t') &\approx -\frac{\mathcal{K}}{3} + \frac{\mathcal{K}}{3} \left[1 + \frac{3A (p_1 p_2 p_3)^{\frac{1-w}{2}}}{2\mathcal{K}^2 \kappa \hbar^2} + \dots \right] \\ &\approx \frac{A}{2\mathcal{K} \kappa \hbar^2} (p_1 p_2 p_3)^{\frac{1-w}{2}}. \end{aligned} \quad (\text{B5})$$

⁸ This is also true for the special cases of vacuum and of scalar matter with $w = 1$, in both of which $p_I c_I = \text{constant}$ and thus $\bar{\mu}_I c_I \propto p_I^{-3/2} \rightarrow 0$ classically. For the case of the cosmological constant ($w = -1$), the cosmological constant Λ has to be very small to admit the semi-classicality.

⁹ The assumption that $\cos(\bar{\mu}_I c_I)$ flip signs at only slightly different moments could be wrong in general. However, note that even if $\cos(\bar{\mu}_I c_I) \approx \cos(\bar{\mu}_J c_J)$ does not hold very well, the vanishing of (B3) is still a good approximation near the bounce, since $(p_1 p_2 p_3)^{(1-w)/2} = a^{3(1-w)} \rightarrow 0$ for $w < 1$ when a is small enough. (But the condition $\cos(\bar{\mu}_I c_I) \approx \cos(\bar{\mu}_J c_J)$ makes the approximation (B3) even more accurate.) In the special case for $w = 1$, (B3) vanishes *exactly* simply because the factor $(1-w)/2$ is zero.

It then follows from (B4) that

$$\begin{aligned} \sin(\bar{\mu}_I c_I) &\approx \kappa \gamma \hbar \frac{\Delta^{1/2}}{p_I^{3/2}} \left\{ \mathcal{K}_I + \frac{A}{2\mathcal{K} \kappa \hbar^2} (p_1 p_2 p_3)^{\frac{1-w}{2}} \right\} \\ &\approx \kappa \gamma \hbar \frac{\Delta^{1/2} \mathcal{K}_I}{p_I^{3/2}}, \end{aligned} \quad (\text{B6})$$

provided

$$\mathcal{K}_I \gg \frac{A}{\mathcal{K} \kappa \hbar^2} (p_1 p_2 p_3)^{\frac{1-w}{2}}. \quad (\text{B7})$$

Taking (B4) into (35) and expressing $\cos x = \pm(1 - \sin^2 x)^{1/2}$ with the help of (B6), we get for instance

$$\begin{aligned} \frac{1}{p_1} \frac{dp_1}{dt'} &\approx \pm \kappa \hbar (\mathcal{K}_2 + \mathcal{K}_3 + \dots) \\ &\quad \times \left[1 - \frac{(\kappa \gamma \hbar)^2 \Delta}{p_1^3} (\mathcal{K}_I + \dots)^2 \right]^{1/2} \\ &\approx \pm \kappa \hbar (\mathcal{K}_2 + \mathcal{K}_3) \left[1 - \frac{p_{1,\text{crit}}^3}{p_1^3} \right]^{1/2}, \end{aligned} \quad (\text{B8})$$

where the critical value $p_{I,\text{crit}}$ is given by the Planck length square ℓ_{Pl}^2 times a numerical factor:

$$\begin{aligned} p_{I,\text{crit}} &:= |\mathcal{K}_I|^{2/3} (\kappa \gamma \hbar)^{2/3} \Delta^{1/3} \\ &\approx 19.01 \gamma |\mathcal{K}_I|^{2/3} \ell_{\text{Pl}}^2. \end{aligned} \quad (\text{B9})$$

Therefore, the big bang singularity is replaced by the bounces whenever each of p_I approaches its critical value $p_{I,\text{crit}}$. The bounces occur up to three times, once in each diagonal direction. If we define the *directional density* ϱ_I in the I -direction as:

$$\varrho_I := \frac{\kappa \hbar^2 \mathcal{K}_I^2}{3p_1^3}, \quad (\text{B10})$$

the above statement can be rephrased to say: The big bounces take place whenever each of the directional densities reaches the critical value

$$\varrho_{\text{crit}} = 3(\kappa \gamma^2 \Delta)^{-1} \approx .82 \rho_{\text{Pl}}. \quad (\text{B11})$$

Note that ϱ_I have the same dimension as ρ_M and moreover we have

$$\kappa^{-1} \frac{\bar{\Sigma}^2}{a^6} = \frac{1}{3} \left[\frac{p_1^3 \varrho_1 + p_2^3 \varrho_2 + p_3^3 \varrho_3}{p^3} \right] \quad (\text{B12})$$

with

$$\bar{\Sigma}^2 := \frac{1}{18} (\alpha_{12}^2 + \alpha_{23}^2 + \alpha_{31}^2) \quad (\text{B13})$$

being identical to the shear factor Σ^2 of the classical solution. This suggests that ϱ_I can be roughly interpreted as the “energy density carried from the classical anisotropic shear portioned for the I -direction” (and thus the name).

To meet the condition (B7) of Case (i), we take the critical values $p_{I,\text{crit}}$ into (B7) and find the criterion for Case (i) to be

$$A \ll \frac{|\kappa_I| \gamma^{w-1}}{|\kappa_1 \kappa_2 \kappa_3|^{(1-w)/3}} \mathcal{K}^{1+w} \kappa^w \hbar^{1+w} \Delta^{\frac{w-1}{2}}. \quad (\text{B14})$$

Next, in Case (ii), on the other hand, the second term in the square bracket of (A6) dominates and we have

$$f(t') \approx \sqrt{\frac{A}{3\kappa\hbar^2}} (p_1 p_2 p_3)^{\frac{1-w}{4}}. \quad (\text{B15})$$

It then follows from (B4) that

$$\sin(\bar{\mu}_I c_I) \approx \kappa \gamma \hbar \frac{\Delta^{1/2}}{p_I^{3/2}} \sqrt{\frac{A}{3\kappa\hbar^2}} (p_1 p_2 p_3)^{\frac{1-w}{4}}, \quad (\text{B16})$$

provided

$$\mathcal{K}_I \gg \frac{A}{\kappa\hbar^2} (p_1 p_2 p_3)^{\frac{1-w}{2}}. \quad (\text{B17})$$

With the help of (B6) again, (35) gives

$$\begin{aligned} \frac{1}{p_1} \frac{dp_1}{dt'} &\approx \pm 2\kappa\hbar \sqrt{\frac{A}{3\kappa\hbar^2}} (p_1 p_2 p_3)^{\frac{1-w}{4}} \\ &\times \left[1 - \frac{(\kappa\gamma\hbar)^2 \Delta}{p_1^3} \frac{A}{3\kappa\hbar^2} (p_1 p_2 p_3)^{\frac{1-w}{2}} \right]^{1/2}. \end{aligned} \quad (\text{B18})$$

The big bang singularity is again replaced by the bounces and the bouncing points of p_I are roughly equal in all three direction; i.e., each p_I is bounced when $p_I \approx p_{\text{crit}}$ with

$$p_{\text{crit}} := \left[\frac{\kappa\gamma^2 \Delta A}{3} \right]^{\frac{2}{3(1+w)}}. \quad (\text{B19})$$

For more generic cases (with multiple matters), this means that the bounces take place near the point when the (total) matter density approaches its critical value

$$\rho_{\text{crit}} \equiv A p_{\text{crit}}^{-3(1+w)/2} = 3(\kappa\gamma^2 \Delta)^{-1} \approx .86\rho_{\text{Pl}}, \quad (\text{B20})$$

begin the same as the critical value given in (B11).

To meet the condition (B17) of Case (ii), we take the critical value p_{crit} into (B17) and find the criterion for Case (ii) to be

$$A \ll \gamma^{w-1} \mathcal{K}_I^{1+w} \kappa^w \hbar^{1+w} \Delta^{\frac{w-1}{2}}, \quad (\text{B21})$$

which is exactly the opposite of the criterion (B14) if we have $\kappa_I \sim \mathcal{O}(1)$.

Finally, in Case (iii), we have

$$A \sim \gamma^{w-1} \mathcal{K}^{1+w} \kappa^w \hbar^{1+w} \Delta^{\frac{w-1}{2}}, \quad (\text{B22})$$

which yields

$$p_{I,\text{crit}} \sim p_{\text{crit}}. \quad (\text{B23})$$

Therefore, in Case (iii), the big bang singularity is replaced by big bounces as well and the bouncing points of p_I are between $p_{I,\text{crit}}$ given by (B9) and p_{crit} given by (B19) ($p_{I,\text{crit}}$ and p_{crit} are now in the same order).

To sum up, the big bang singularity is replaced by big bounces due to the fact that the gravity with loop quantum corrections becomes repulsive at some point when the universe is near the singularity. In Cases (i), this happens when the directional density ϱ_I reaches Planckian energy density $.86\rho_{\text{Pl}}$; in Case (ii), it happens when the matter density ρ_M approaches $\approx .86\rho_{\text{Pl}}$. In all cases, the big bounce takes place whenever either of ϱ_I or ρ_M approaches $\mathcal{O}(\rho_{\text{Pl}})$ first. In a sense, there is competition between the energy density carried from the classical anisotropic shear (ϱ_I) and the matter density (ρ_M) to be the indication of occurrence of the big bounces.

Also notice that as mentioned in Section III, $\Sigma^2(\text{post bounce}) \neq \Sigma^2(\text{pre bounce})$ in general due to the fact that the anisotropies are smeared by the quantum corrections. However, in Case (i), the information of anisotropies persists during the bouncing period and we shall have $\Sigma^2(\text{post bounce}) \approx \Sigma^2(\text{pre bounce})$. This can be seen from (B8), in which the evolutions for different p_I are decoupled around the bounces and therefore the constants \mathcal{K}_I (which dictate anisotropies) are unchanged before and after the bounce.

The equations of motion given by (35) and (36) can be solved numerically once the initial values $p_I(t=t_0)$ and $c_I(t=t_0)$ are given. Equivalently, for given $p_I(t_0)$, specifying \mathcal{K}_I is an alternative way to specify $c_I(t_0)$. [Given \mathcal{K}_I , $f(t_0)$ can be obtained via (A6) and then $c_I(t_0)$ are fixed by (A1) if the initial condition is in the classical regime and by (B4) if in quantum regime.] By changing the parameters A and \mathcal{K} , we can get the three different cases as discussed above. The numerical solutions in the presence of radiation are solved in terms of proper time t and depicted in Figures 8, 9 and 10 for these three cases respectively.

APPENDIX C: ALTERNATE QUANTIZATION

In this section we consider the effective dynamics of an alternative quantization scheme mentioned in Sec-

tion III. The major difference is that the behavior of the parameters $\bar{\mu}_I$ varies with the triad components differently. Specifically we take the dependence as $\bar{\mu}_I \propto 1/a_I$

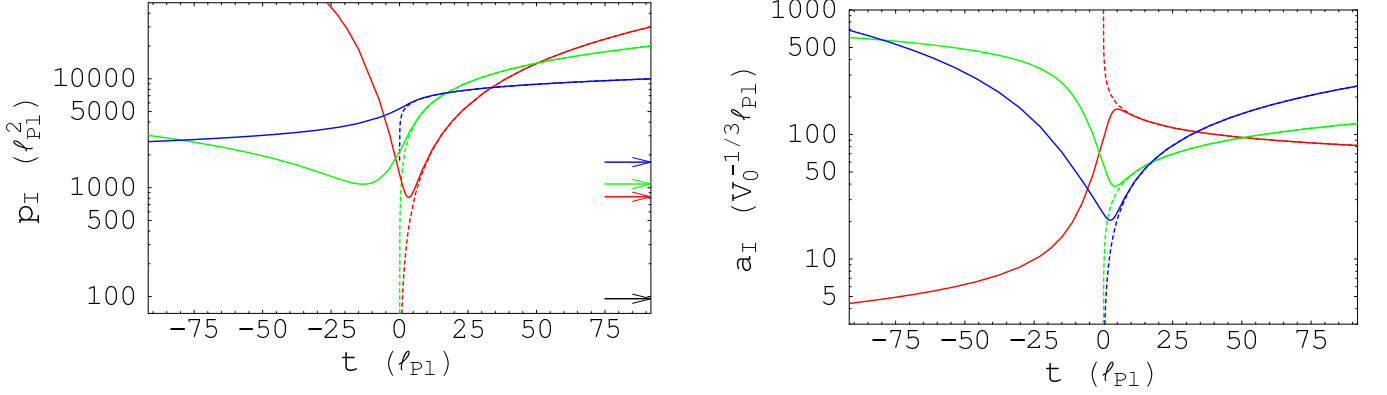


FIG. 8: **Case (i): Quantum corrections take effect in the Kasner phase.** With $w = 1/3$ (radiation filled); $\kappa_1 = -2/7$, $\kappa_2 = 3/7$, $\kappa_3 = 6/7$; $\mathcal{K} = 1. \times 10^3$; $A = 1. \times 10^2 \hbar \ell_{\text{Pl}}^{3w-1}$; and $p_1(t_0) = 3. \times 10^4 \ell_{\text{Pl}}^2$, $p_2(t_0) = 2. \times 10^4 \ell_{\text{Pl}}^2$, $p_3(t_0) = 1. \times 10^4 \ell_{\text{Pl}}^2$. (Also set $\gamma = 1$.) The red curves are for p_1 , a_1 ; green for p_2 , a_2 ; and blue for p_3 , a_3 . Solid lines are the solution to the effective loop quantum evolution; dashed lines to the classical evolution. The proper time t is offset such that the classical singularity is at the origin of t . The values of $p_{I,\text{crit}}$ are pointed by the colored arrows and p_{crit} by the black one. In this case, the bouncing point of each p_I matches $p_{I,\text{crit}}$ very precisely and we have $p_{I,\text{crit}} \gg p_{\text{crit}}$ (or say $\varrho_I \ll \rho_M \sim \rho_{\text{Pl}}$ near the bounces). [Note that the bounce of p_3 is out of the shown range. The isotropized phases on both sides of the bounces are also out of plot.]

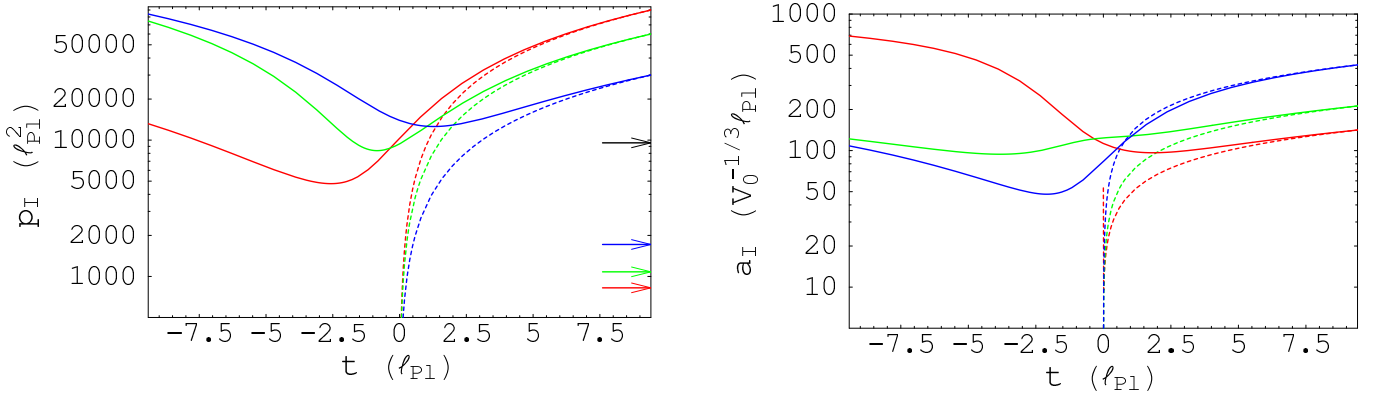


FIG. 9: **Case (ii): Quantum corrections take effect in the isotropized phase.** With $w = 1/3$ (radiation filled); $\kappa_1 = -2/7$, $\kappa_2 = 3/7$, $\kappa_3 = 6/7$; $\mathcal{K} = 1. \times 10^3$; $A = 1. \times 10^6 \hbar \ell_{\text{Pl}}^{3w-1}$; and $p_1(t_0) = 9. \times 10^4 \ell_{\text{Pl}}^2$, $p_2(t_0) = 6. \times 10^4 \ell_{\text{Pl}}^2$, $p_3(t_0) = 3. \times 10^4 \ell_{\text{Pl}}^2$. In this case, the bouncing point of each p_I roughly matches p_{crit} and we have $p_{I,\text{crit}} \ll p_{\text{crit}}$ (or say $\varrho_I \ll \rho_M \sim \rho_{\text{Pl}}$ near the bounces). [Note that in the backward evolution the contracting curve of the classical a_1 eventually becomes expanding at the epoch extremely close to the singularity, indicating that the Kasner phase does occur classically although almost invisible in the plot.]

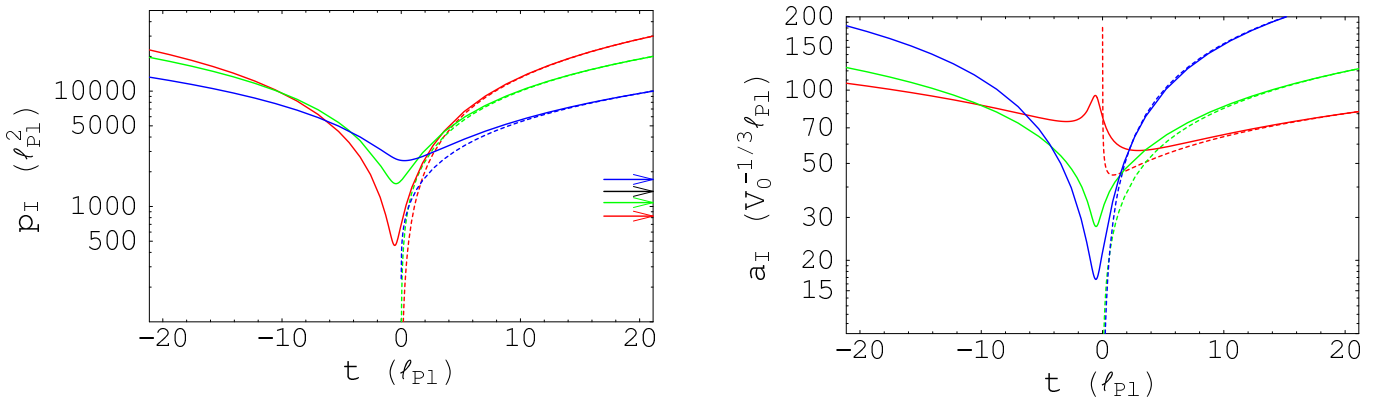


FIG. 10: **Case (iii): Quantum corrections take effect in the transition phase.** With $w = 1/3$ (radiation filled); $\kappa_1 = -2/7$, $\kappa_2 = 3/7$, $\kappa_3 = 6/7$; $\mathcal{K} = 1. \times 10^3$; $A = 2. \times 10^4 \hbar \ell_{\text{Pl}}^{3w-1}$; and $p_1(t_0) = 3. \times 10^4 \ell_{\text{Pl}}^2$, $p_2(t_0) = 2. \times 10^4 \ell_{\text{Pl}}^2$, $p_3(t_0) = 1. \times 10^4 \ell_{\text{Pl}}^2$. In this case, we have $p_{I,\text{crit}} \sim p_{\text{crit}}$, roughly around which all p_I are bounced (or say $\varrho_I \sim \rho_M \sim \rho_{\text{Pl}}$ near the bounces).

with the exact behavior for $\bar{\mu}_1$ given as

$$\bar{\mu}_1 = \sqrt{\frac{\Delta p_1}{p_2 p_3}}. \quad (\text{C1})$$

The effective Hamiltonian is similar in form to that in (34) and is given explicitly by

$$\mathcal{H}_{\text{eff}} = -\frac{1}{\kappa\gamma^2} \left\{ \frac{\sin(\bar{\mu}_2 c_2) \sin(\bar{\mu}_3 c_3)}{\bar{\mu}_2 \bar{\mu}_3} p_2 p_3 + \text{cyclic terms} \right\} + p_1 p_2 p_3 \rho_M, \quad (\text{C2})$$

which becomes

$$\mathcal{H}_{\text{eff}} = -\frac{p_1 p_2 p_3}{\kappa\gamma^2 \Delta} \left\{ \sin(\bar{\mu}_2 c_2) \sin(\bar{\mu}_3 c_3) + \text{cyclic terms} \right\} + p_1 p_2 p_3 \rho_M. \quad (\text{C3})$$

With this, the vanishing of the constraint leads to the simple relation

$$\rho_M = \frac{1}{\kappa\gamma^2 \Delta} \left\{ \sin(\bar{\mu}_2 c_2) \sin(\bar{\mu}_3 c_3) + \text{cyclic terms} \right\}$$

and from this we can deduce an important observation. Namely, since all of the sin terms are bounded we find that the energy density is also bounded as

$$\rho_M < \frac{3}{\kappa\gamma^2 \Delta} \equiv \rho_{\text{crit}}, \quad (\text{C4})$$

where ρ_{crit} is numerically the same value as in the isotropic case

$$\rho_{\text{crit}} \equiv \frac{3}{\kappa\gamma^2 \Delta} \approx .82\rho_{\text{Pl}}. \quad (\text{C5})$$

The fact that ρ_M is bounded implies that the big-bang singularity is resolved since classically the energy density blows up there. Note that any bounce does not necessarily occur when $\rho_M = \rho_{\text{crit}}$ and we shall see, that with anisotropies the bounce occurs at lower energy densities.

We can derive Hamilton's equations in the same fashion as in Section III and it can be shown that

$$p_I c_I - p_J c_J = \gamma V_0 \alpha_{IJ}, \quad (\text{C6})$$

where α_{IJ} are constants of motion. Note that this exact relation was satisfied in the classical case in (19). However, with this effective Hamiltonian, c_I are not as simply related to \dot{a}_I as in the classical case given in (15). The full relation is to be determined from the Hamilton's equation for \dot{p}_I which give for instance

$$\dot{p}_1 = \frac{p_1}{\sqrt{\Delta}\gamma} \cos(\bar{\mu}_1 c_1) \left(\sin(\bar{\mu}_2 c_2) + \sin(\bar{\mu}_3 c_3) \right). \quad (\text{C7})$$

Because of this, the shear term $\Sigma^2 = \frac{a^6}{18} [(H_1 - H_2)^2 + (H_2 - H_3)^2 + (H_3 - H_1)^2]$ is no longer constant. However,

in the classical limit where $\bar{\mu}_I c_I \ll 1$, we can calculate the shear term to be $\Sigma^2 \approx \frac{1}{18} (\alpha_{12}^2 + \alpha_{23}^2 + \alpha_{31}^2)$ as in the classical case.

Therefore if we consider the behavior of the shear term and begin with a semi-classical collapsing universe, we find that initially Σ^2 is constant with value

$$\Sigma^2 \approx \bar{\Sigma}^2 \equiv \frac{1}{18} (\alpha_{12}^2 + \alpha_{23}^2 + \alpha_{31}^2). \quad (\text{C8})$$

Through the bounce Σ is not constant, but after the bounce in the expanding phase where once again $\bar{\mu}_I c_I \ll 1$, we find that the shear takes on the same value. This is because equation (C6) holds throughout the evolution. Therefore it is a rather general feature of this effective Hamiltonian, that the shear term Σ is conserved before and after the collision. Note that this is in contrast with the results presented in the body of this paper, where Σ was only conserved for a massless scalar field. However, both quantizations imply that the shear term is bounded and the anisotropies do not blow up.

Because of the complexity of the equations of motion, it is highly non-trivial to derive a generalized Friedmann equation. We can however if we expand the effective Hamiltonian to second order in $\bar{\mu}_I c_I$. Then equations (C6) and (C7) can be used to derive an approximate generalized Friedmann equation given by

$$H^2 = \frac{\kappa}{3} \rho_M \left(1 - \frac{\rho_M}{\rho_{\text{crit}}} \right) + \frac{\bar{\Sigma}^2}{a^6} - \frac{3\bar{\Sigma}^2 \rho_M}{a^6 \rho_{\text{crit}}} - \frac{9\bar{\Sigma}^4}{\kappa a^{12} \rho_{\text{crit}}} + \mathcal{O}((\bar{\mu}_I c_I)^4). \quad (\text{C9})$$

If we solve this for the matter energy density at the bounce ($H = 0$) we find

$$\rho_{\text{bounce}} \approx 1/2 \left(\rho_{\text{crit}} - \frac{9\bar{\Sigma}^2}{\kappa a^6} + \sqrt{(\rho_{\text{crit}} - \frac{9\bar{\Sigma}^2}{\kappa a^6})(\rho_{\text{crit}} - \frac{3\bar{\Sigma}^2}{\kappa a^6})} \right), \quad (\text{C10})$$

which implies that the energy density is bounded below ρ_{crit} in accordance with the prediction from the vanishing of the effective Hamiltonian. Note that $\bar{\Sigma}^2$ is a constant of motion and only related to the shear term Σ^2 in the classical limit $\bar{\mu}_I c_I \ll 1$. Note also, that this generalized Friedmann equation is valid in the nearly isotropic limit which can be understood from the relations (C6) which imply

$$\bar{\mu}_I c_I - \bar{\mu}_J c_J = \frac{\gamma \sqrt{\Delta} \alpha_{IJ}}{a^3}. \quad (\text{C11})$$

If the right hand side is not small (i.e., when the anisotropies are large), then at least one $\bar{\mu}_I c_I$ is guaranteed to be large and hence the generalized Friedmann equation would need to be calculated to higher order to provide a good approximation.

We note that both the quantization scheme presented in this appendix and that given in the body of this work agree as to the qualitative nature of the bouncing universe. Namely, a bounce still occurs with the inclusion

of anisotropies and that the shear term does not blow up implying that the anisotropies remain finite through the bounce.

-
- [1] M. Bojowald. Loop quantum cosmology. *Living Rev. Rel.*, 8:11, 2005.
- [2] A. Ashtekar, T. Pawłowski, and P. Singh. Quantum nature of the big bang. *Phys. Rev. Lett.*, 96:141301, 2006.
- [3] A. Ashtekar, T. Pawłowski, and P. Singh. Quantum nature of the big bang: An analytical and numerical investigation I. *Phys. Rev.*, D73:124038, 2006.
- [4] A. Ashtekar, T. Pawłowski, and P. Singh. Quantum nature of the big bang: Improved dynamics. *Phys. Rev.*, D74:084003, 2006.
- [5] A. Ashtekar, T. Pawłowski, P. Singh, and K. Vandersloot. Loop quantum cosmology of $k=+1$ FRW models. *Phys. Rev.*, D75:024035, 2007.
- [6] K. Vandersloot. Loop quantum cosmology and the $k = -1$ RW model. *Phys. Rev.*, D75:023523, 2007.
- [7] P. Singh, K. Vandersloot, and G. V. Vereshchagin. Non-singular bouncing universes in loop quantum cosmology. *To appear in Phys. Rev. D*, 2006.
- [8] M. Bojowald, H. Hernandez, M. Kagan, P. Singh, and A. Skirzewski. Hamiltonian cosmological perturbation theory with loop quantum gravity corrections. *Phys. Rev.*, D74:123512, 2006.
- [9] M. Bojowald. Loop quantum cosmology and inhomogeneities. *Gen. Rel. Grav.*, 38:1771–1795, 2006.
- [10] M. Bojowald, H. Hernandez, M. Kagan, and A. Skirzewski. Effective constraints of loop quantum gravity. *Phys. Rev.*, D75:064022, 2007.
- [11] M. Bojowald, H. Hernandez, M. Kagan, P. Singh, and A. Skirzewski. Formation and evolution of structure in loop cosmology. *Phys. Rev. Lett.*, 98:031301, 2007.
- [12] M. Bojowald. Homogeneous loop quantum cosmology. *Class. Quant. Grav.*, 20:2595–2615, 2003.
- [13] D. Chiou. Loop quantum cosmology in Bianchi I models: Analytical investigation. *Phys. Rev.*, D75:024029, 2007.
- [14] A. Ashtekar, M. Bojowald, and J. Lewandowski. Mathematical structure of loop quantum cosmology. *Adv. Theor. Math. Phys.*, 7:233–268, 2003.
- [15] M. Bojowald. Large scale effective theory for cosmological bounces. *Phys. Rev.*, D74:081301, 2007.
- [16] K. Vandersloot. On the Hamiltonian constraint of loop quantum cosmology. *Phys. Rev.*, D71:103506, 2005.
- [17] Magueijo J and P. Singh. Thermal fluctuations in loop cosmology. *astro-ph/0703566*.
- [18] A. Perez. On the regularization ambiguities in loop quantum gravity. *Phys. Rev.*, D73:044007, 2006.
- [19] K. Vandersloot. Loop quantum cosmology. Ph.D. Dissertation, The Pennsylvania State University (2006).